Title
Networks of High Aspect Ratio Particles to Direct Colloidal Assembly Dynamics and Cellular Interactions

Permalink
https://escholarship.org/uc/item/0j0007sx

Authors
Finbloom, Joel A
Demaree, Benjamin
Abate, Adam R
et al.

Peer reviewed

Networks of High Aspect Ratio Particles to Direct Colloidal Assembly Dynamics and Cellular Interactions

Joel A. Finbloom, **Benjamin Demaree**, **Adam R. Abate**, **Tejal A. Desai**
Department of Bioengineering and Therapeutic Sciences, University of California, San Francisco. San Francisco, CA 94158

Abstract

Injectable colloids that self-assemble into three-dimensional networks are promising materials for applications in regenerative engineering, as they create open systems for cellular infiltration, interaction, and activation. However, most injectable colloids have spherical morphologies, which lack the high material-biology contact areas afforded by higher aspect ratio materials. To address this need, injectable high aspect ratio particles (HARPs) were developed that form three-dimensional networks to enhance scaffold assembly dynamics and cellular interactions. HARPs were functionalized for tunable surface charge through layer-by-layer electrostatic assembly. Positively charged Chitosan-HARPs had improved particle suspension dynamics when compared to spherical particles or negatively charged HARPs. Chit-HARPs were used to improve the suspension dynamics and viability of MIN6 cells in three-dimensional networks. When combined with negatively charged gelatin microsphere (GelMS) porogens, Chit-HARPs reduced GelMS sedimentation and increased overall network suspension, due to a combination of HARP network formation and electrostatic interactions. Lastly, HARPs were functionalized with fibroblast growth factor 2 (FGF2) to highlight their use for growth factor delivery. FGF2-HARPs increased fibroblast proliferation through a combination of 3D scaffold assembly and growth factor delivery. Taken together, these studies demonstrate the development and diverse uses of high aspect ratio particles as tunable injectable scaffolds for applications in regenerative engineering.

Graphical Abstract:

High Aspect Ratio Particles (HARPs) are fabricated from polycaprolactone and functionalized via layer-by-layer (LbL) assembly with chitosan and heparin to develop injectable colloidal scaffolds. HARPs form entangled networks with improved suspension dynamics compared to spherical particles. HARPs can be used to improve cellular dynamics and viability, facilitate mixed particle co-assemblies, and initiate growth factor delivery for regenerative engineering applications.

Tejal.Desai@ucsf.edu.

1. Introduction

Synthetic materials that interact with biological systems and drive cellular behavior have seen extensive use in regenerative engineering applications. Three-dimensional scaffolds through which cells can infiltrate are particularly beneficial, as the material-biology interface can be engineered to interact with cells for applications including therapeutic cellular delivery and endogenous cell recruitment and activation.[1–6] While the majority of reported scaffolds are bulk hydrogels or macroscale materials that require implantation, injectable scaffolds offer significant benefits in ease of delivery.[5,7] Shear-thinning hydrogels offer one means of developing injectable scaffolds;[8–10] however, hydrogels typically lack microscale porosity and create closed scaffold systems that interact with the surrounding tissue environment only along the hydrogel exterior. In contrast, microporous scaffolds that are open to the surrounding tissue environments allow for endogenous cell recruitment throughout the entirety of the scaffold, which is important for tissue remodeling or immunomodulatory applications.[11–13] Additionally, porous scaffold systems offer advantages for creating three-dimensional cellular suspensions, where cells can receive nutrients from the surrounding environment, interact with one another, and form connections to improve viability and functional outputs.[4,12–16]

Colloids that assemble into three-dimensional networks are promising materials to create cellular scaffolds, as they are injectable and create open porous systems, where the architecture of the scaffold is controlled by the colloid properties and self-assembly dynamics.[7,17–19] Further, colloidal scaffolds offer advantages in modularity, as individual particle populations can be combined to create complex environments with multiple functionalities to better recapitulate the extracellular matrix or to activate multiple cell types in a single scaffold.[1] Hydrogel microparticles, or microgels, have been the material of choice for these self-assembling scaffolds and shown promise for both three-dimensional cell culture, as well as injectable materials for local tissue remodeling.[1,11,20] However, microgel scaffold assembly primarily relies on gravitational packing parameters of individual microgel components, which are almost exclusively spherical particles.[20] This limits the surface area to volume ratio of the microgel scaffolds, which is an important parameter to maximize particle-cell interactions.[21,22] Additionally, most colloidal scaffolds still rely on crosslinking chemistries between the particles, or on being embedded within macroscale hydrogel networks in order to maintain their three-dimensional architectures. [1,11,12,23] This limitation is again likely due to the spherical morphology of most colloidal hydrogel systems. Electrospun nanofiber meshes provide high surface area to volume ratios and have been used extensively for tissue engineering; however, these nanofiber networks must be implanted and are therefore limited in their broad applicability.[24–27]

High aspect ratio particles (HARPs) are an emerging class of materials with unique properties that combine the strengths of nanofiber meshes with injectable particle systems. HARPs provide a high surface area to volume ratio, which can maximize local cellular interactions within the scaffold, while providing an open system for cellular recruitment and activation. Research into the effects of particle aspect ratio on biomedical functionality have primarily focused on particle biodistribution and drug delivery.[21,22,28–31] The aspect ratio of particles could also influence colloid assembly dynamics and therefore affect scaffold architecture and resultant regenerative engineering functionalities,[5,19] although such particle structure-activity relationships remain poorly understood.

We have previously shown that injectable rod-shaped microgels fabricated from polyethylene glycol or hyaluronic acid can attenuate fibrotic phenotypes in fibroblasts and improve cardiac repair following myocardial infarction in rat models.[32,33] However, these microrods do not assemble into scaffolds within the injection space, likely owing to their large size and moderate aspect ratio (15×100 μm, Aspect Ratio = 6.67). We recently reported a new class of "nanowire" high aspect ratio particles (0.2×20 μm, Aspect Ratio = 100). These HARPs were fabricated from biodegradable polycaprolactone (PCL) using a nanotemplating approach, conjugated to antibodies for endogenous cytokine binding, and were injected subcutaneously for local immunomodulation.[34,35] Importantly, these HARPs are on the same length scale as cells, and thus facilitate maximal material-cell contact along the longitudinal axis of the HARPs.

In this work, we report on the development of polycaprolactone HARPs as injectable colloidal scaffolds to direct particle assembly dynamics and influence cellular interactions for applications in regenerative engineering. We first sought to better understand the influence of physicochemical colloidal properties such as particle shape and surface charge on scaffold assembly in order to maximize particle stability and cellular interactions. Using layer-by-layer (LbL) electrostatic assembly, HARPs were functionalized with biopolymers such as chitosan to enhance scaffold suspension dynamics and increase cellular interactions. We found that HARPs have tunable assembly dynamics and self-assemble to form mesh-like networks with bridging stabilization between individual particles. By engineering the physicochemical properties of PCL HARPs, we improved the suspension dynamics and viability of cellular cargo, facilitated the co-assembly of mixed particle scaffolds composed of HARPs and microspheres, and functionalized HARPs with growth factors to promote cellular infiltration and proliferation. These findings demonstrate that not only are HARPs promising injectable scaffolds for regenerative engineering and tissue remodeling, but that the physicochemical properties of colloids offer exciting engineering opportunities to improve the materials-biology interface of injectable scaffolds.

2. Results and Discussion

2.1. HARP Fabrication, Functionalization, and Suspension Behavior

High aspect ratio particles were fabricated from polycaprolactone (PCL) using a previously reported nano-templating technique.[34] HARPs were formed after polymer melting and capillary flow into the pores of an anodized aluminum oxide template, followed by template etching in alkaline solution and HARP purification (Figure S1). This method afforded

HARPs of ~20 μm in length and 200 nm in diameter. Additionally, hydrophobic fluorescent cargo such as Nile red dye can be encapsulated into the PCL core of the HARPs. This fluorescent cargo is maintained over the course of weeks within the HARPs and can be imaged via fluorescence microscopy or for analysis of *in vivo* tissue retention of HARPs. [34,35] Zeta potential analysis of HARPs revealed a highly negative charged surface, likely owing to the alkaline etching step within the fabrication process (Figure 1a,b). Alkaline treatment of PCL materials has previously been used to hydrolyze the ester backbone of PCL and expose negatively charged carboxylate moieties.[36,37] We capitalized on this negative charge to facilitate layer-by-layer (LbL) electrostatic assembly of biopolymers onto HARPs (Figure 1a). LbL provides a facile and robust method to functionalize particles with diverse polymers or bioactive cargo, and has been used in previous applications of drug delivery and tissue engineering.[38] Chitosan and heparin were chosen as model biomaterials to demonstrate the functionalization of HARP surfaces with positively or negatively charged biopolymers, respectively. Chitosan and heparin are widely used biomaterials for regenerative engineering applications, as chitosan can increase tissue retention and overall biocompatibility of materials, while the high binding affinity of heparin to various growth factors has been utilized for growth factor delivery.[39,40] To confirm the LbL functionalization of HARPS, the surface charge of HARPs was monitored prior to functionalization, as well as after incubations with chitosan and heparin biopolymers (Figure 1b). We observed charge oscillations following each step of electrostatic assembly, demonstrating that HARPs serve as suitable materials for LbL functionalization.

For applications involving injectable colloidal scaffolds, it is imperative to assess the suspension dynamics of the colloidal materials under study. We hypothesized that particle physicochemical properties such as aspect-ratio and surface charge will influence colloid suspension dynamics in solution. To assess this in the context of PCL particles, PCL microspheres were fabricated with diameters of 1.26 ± 0.13 μm, as measured by dynamic light scattering. Following fabrication, PCL spheres were treated with alkaline solution to instill a negatively charged surface (Figure S2). LbL assembly was used to generate positively charged chitosan-coated PCL microspheres or HARPs. The distribution behavior of the particles in PBS solution was monitored using confocal fluorescence microscopy of particles containing Nile red fluorophores (Figure 1c, Figure S3). After 6 h incubation, we observed sedimentation of both positively and negatively charged PCL microspheres, while HARPs of both negative and positive charge demonstrated increased suspension behaviors (Figure 2a). This is likely due to the formation of bridging connections between HARPs, which can form net-like structures to facilitate greater suspension and decrease sedimentation.[19] Indeed, microscopic analysis of HARP structures revealed increased particle interactions and the formation of assembled networks in solution (Figure 2b). Interestingly, chitosan-HARPs displayed increased distribution across the z-axis of the solution when compared to negatively charged unmodified HARPs. This may be the result of several factors, including increased hydrogen-bonding between chitosan polymers on interacting HARPs,[41] as well as possible electrostatic screening of chitosan residues by the phosphate ions in PBS.[42,43] Thus, chitosan-HARPs show promise in improving suspension distribution behaviors when compared to spherical particles or negatively charged HARPs, indicating the importance of physicochemical parameters in the development of colloidal

scaffolds. As chitosan-HARPs demonstrated improved suspension behaviors and chitosan has been used extensively to increase biocompatibility of materials, we sought to develop chitosan-HARPs as injectable colloidal scaffolds for increasing cellular interactions and activation.

2.2. Formation of Cellular Suspensions with HARP Scaffolds

The delivery of cellular cargo has immense potential to advance the fields of tissue engineering and regenerative medicine. For cellular delivery applications, it is important to maintain cellular suspension behaviors in the material scaffold, as cellular sedimentation and aggregation can reduce viability and impair cellular activity.[3,5] Further, porous architectures within cell delivery scaffolds can facilitate cellular communication and activation. Previous work by our lab demonstrated the use of macroscale implantable PCL devices for the encapsulation and delivery of insulin-producing MIN6 cells and pancreatic islets.[16,44] However, it would be advantageous to create a cell delivery scaffold that can be injected, rather than implanted. We were therefore interested in developing HARP scaffolds to improve cellular suspension behaviors for applications in therapeutic cell delivery (Figure 3a). We investigated these assembly dynamics with the model MIN6 cell line, which we had previously engineered to express cytosolic mCherry for cell tracking and viability measurements.[44] MIN6-mCherry cells were suspended in a solution of Chitosan-HARPs, and the distribution of MIN6 cells was monitored with confocal fluorescence microscopy over 3 days. MIN6 cells on their own sedimented to the bottom of the well plate to form a 2D cell culture, with no cells observed above 100 μm from the well bottom (Figure 3b,d). In contrast, MIN6 cells in the Chit-HARP scaffold displayed improved suspension behaviors, with cells observed from 20–250 μm from the well bottom (Figure 3b,d). We hypothesize that this is due to a combination of HARP network formation and electrostatic interactions between positively charged Chit-HARPs and negatively charged cells.

In addition to increasing MIN6 distribution, mCherry fluorescence of MIN6 cells was increased by almost 3-fold in Chit-HARP scaffolds when compared to 2D culture, indicating enhanced viability of MIN6 cells within the scaffold (Figure 3c). Lastly, while MIN6 cells cultured without Chit-HARPs showed significant aggregation by 3 d (Figure 3d), no aggregation behavior was observed for MIN6 cells cultured in Chit-HARP scaffolds (Figure 3d). Thus, Chit-HARPs show promise as scaffolds to increase cellular suspension dynamics and cell viability.

2.3. HARPs as Scaffolds for Colloidal Co-Assemblies

The generation and delivery of mixed particle co-assemblies has been explored to improve the biodistribution and tissue retention of drug carriers and to deliver multiple cargo types with independent release rates.[11,45,46] However, the generation of injectable mixed colloidal assemblies with controlled particle suspension dynamics remains a challenge. Based on our results developing MIN6-HARP cellular suspensions, we hypothesized that HARPs could serve as colloidal scaffolds to improve the suspension dynamics of mixed particle systems through HARP network formation and electrostatic interactions between positively charged Chit-HARPs and negatively charged microspheres. As an initial test of this concept, negatively charged microspheres made of poly(lactic-co-glycolic acid) (PLGA)

were incubated with Chit-HARPs. Strong network formation between PLGA microspheres and Chit-HARPs was observed at pH 7.4, while limited interactions were observed upon increased protonation of both Chit-HARP amines and PLGA carboxylates at pH 5 (Figure S5), indicating that electrostatics play an important role in HARP network formation and particle co-assembly.

We next developed a mixed particle co-assembly system between HARPs and gelatin microsphere hydrogels. Crosslinked gelatin hydrogels have been used extensively in tissue engineering applications.[47,48] In contrast, non-crosslinked gelatin microspheres (GelMS) dissolve at 37 °C over the course of 1–3 days, and thus have much faster release profiles than drugs encapsulated within other types of polymeric particles.[13] We were additionally interested in using GelMS with our co-assembly system, as we hypothesized that GelMS could serve as porogens within HARP scaffolds to maintain a porous architecture over extended periods of time (Figure 4a). After co-assembly with Chit-HARPs, GelMS porogens would dissolve at 37 °C and the soluble gelatin strands would initiate electrostatic crosslinks between adjacent Chit-HARPs to improve suspension dynamics. While GelMS porogens have been explored for the development of porous hydrogel scaffolds,[13] they have not been developed for use in injectable mixed colloidal systems.

Soluble gelatin polymers were labeled with fluorescein-NHS esters and gelatin microspheres were fabricated using a microfluidic dropmaker[49,50] to create monodisperse GelMS of 55 μm diameters and surface charges of −28.9 ± 3.1 mV (Figure S6). After mixing Chit-HARPs and GelMS together in PBS and incubating for 3 h, we observed network formation between HARPs and GelMS (Figure 4b), as well as increased GelMS distribution in the z-axis (Figure 4c). Gelatin microspheres on their own sedimented to the bottom of the well, in agreement with our observations of spherical particle suspension dynamics (Figure 2a). Z-axis GelMS distribution was increased within HARP scaffolds, and even more so within Chit-HARP scaffolds, owing to the combination of HARP network formation and electrostatic interactions between oppositely charged GelMS and Chit-HARPs. To further assess the assembly dynamics of this mixed particle system, the xy areas occupied by GelMS were calculated for representative distances from the well bottom (Figure 4d). Chit-HARPs facilitated more spacious GelMS particle distribution within the xy plane, as well as more homogenous xy GelMS distribution, with a range of ~15–30% xy area occupied across the z axis, which is important for increasing the overall homogeneity of mixed particle systems. GelMS dissolution was observed after 24 h incubation at 37 °C, and the porous Chit-HARP network was maintained after dissolution (Figure 4e). After 3 d incubation of HARP-GelMS co-assemblies at 37 °C, Chit-HARPs maintained excellent macroscopic suspension dynamics, whereas negatively charged HARPs sedimented to the bottom (Figure 4f), indicating the importance of electrostatic interactions and dissolved gelatin crosslinks in this co-assembled system.

2.4. Growth Factor Delivery with HARP-Porogen Co-Assemblies

Growth factors are commonly used cargos for improving wound healing and regenerative outcomes by activating endogenous repair mechanisms.[40] While direct growth factor injection suffers from poor distribution and biological half-life, immobilization and

subsequent delivery of growth factors from biomaterial scaffolds has seen success in increasing growth factor activity.[40] It has also been observed that the porosity of biomaterial scaffolds is an important design parameter to enable efficient endogenous cellular infiltration and activation.[1,4,12] As the majority of growth factor delivery scaffolds are either implantable materials or injectable hydrogels, Chit-HARPs could provide a new approach to growth factor delivery by enabling colloidal scaffold injection, cellular infiltration, and growth factor-mediated activation for regenerative engineering. This application would benefit from the co-assembly system developed between Chit-HARPs and GelMS porogens, as the increased porosity and suspension dynamics could improve cellular infiltration and activation within the scaffold network.

To develop Chit-HARPs as scaffolds for growth factor delivery, fibroblast growth factor 2 (FGF2) was chosen as a model growth factor cargo, as FGF2 has been used extensively in delivery applications and has shown efficacy in improving wound healing.[40] Additionally, FGF2 has a high binding affinity for heparin, which can be attached onto Chit-HARPs through layer-by-layer assembly (Figure 1b). To attach FGF2 onto HARPs, Chit-HARPs were first fabricated, followed by the pre-incubation of heparin with FGF2. This pre-incubation allowed for binding of heparin to the growth factor, while the negatively charged heparin served to anchor the protein onto positively charged Chit-HARPs (Figure 5a). Incubation of FGF2 with heparin and subsequent addition to Chit-HARPs led to FGF2 loading efficiencies of over 50%. Release studies revealed first order release of FGF2 from HARPs, with slowed FGF2 release rates upon addition of a chitosan layer onto the FGF2-HARPs (Figure 5b). This is in agreement with literature reports, which demonstrate that as the number of electrostatic layers increases on top of adsorbed cargo, release rates slow, enabling tunable release rates depending on the desired application.[38]

To assess cell infiltration and proliferation within HARP scaffolds, NIH-3T3 fibroblasts were used as a model cell line. FGF2-HARPs were combined with Chit-HARPs and GelMS porogens and pre-incubated for 1 d at 37 °C to allow for GelMS dissolution and scaffold formation. After this pre-incubation of scaffolds and control groups, fibroblasts were added, and proliferation was monitored after 3 d using a Cyquant proliferation assay (Figure 5c). We observed ~1.5-fold proliferation of fibroblasts cultured in Chit-HARP+GelMS co-assemblies compared to untreated and FGF2-treated cells. This result is in agreement with our previous findings related to MIN6 growth within HARP scaffolds, as the HARP+GelMS scaffolds provide three-dimensional space for increased cell proliferation. FGF2 did not have significant effects on fibroblast proliferation, likely owing to the 24 h pre-incubation and the short half-life of FGF2 in cell culture conditions.[51,52] However, when FGF2 was immobilized onto HARPs and combined with Chit-HARPs+GelMS co-assemblies, fibroblast proliferation was increased ~2.5-fold, indicating increased stability and activity of FGF2 via heparin-mediated immobilization onto HARP scaffolds. Thus, Chit-HARP+GelMS co-assemblies not only show promise as stand-alone scaffolds for increased cell proliferation but can be functionalized with bioactive growth factors for improved growth factor stabilization, controlled release, and increased cellular activation.

3.   Conclusion

The development of biomaterial-based scaffolds for cellular delivery and endogenous cellular activation is an important avenue of research to enhance regenerative medicine. While previous research efforts have focused on implantable materials and hydrogels, we developed a new approach, which relied on physiochemical engineering of injectable high aspect ratio particles (HARPs) to improve cellular suspension dynamics and activation. We demonstrated that the physicochemical parameters of colloidal materials such as surface charge and aspect ratio play important roles in directing particle assembly behaviors and suspension dynamics. We further took advantage of these parameters to develop HARPs as scaffolds to improve cellular infiltration and viability, and to drive the assembly of mixed particle systems for the enhanced activation and proliferation of fibroblasts via scaffold-mediated growth factor delivery. Taken together, these studies highlight the diverse uses of high aspect ratio particles as injectable scaffolds for applications in regenerative engineering.

4.   Experimental Section/Methods

4.1.   General Methods and Instrumentation:

Unless otherwise noted, all reagents were purchased from commercial sources. 45 kD PCL was used for the fabrication of HARPs. 15 kD PCL was used for formation of PCL spheres. Gelatin Type B was purchased from Sigma Aldrich (St. Louis, MO). Low molecular weight chitosan was purchased from Sigma Aldrich (St. Louis, MO), and was 90% deacylated according to the manufacturer. Low molecular weight heparin sodium salt was purchased from Tocris (Minneapolis, MN), and was stored under desiccation. All reagent solutions were freshly prepared for each experiment and fabrication process.

Zeta potential and dynamic light scattering measurements were conducted on a Malvern Zetasizer DS90. Absorbance and fluorescence quantification measurements were conducted on a Molecular Devices SpectraMax M5 plate reader. All microscopy studies were conducted at the UCSF Nikon Imaging Center using a Nikon Ti spinning disk confocal microscope.

4.2.   Particle Fabrication:

High aspect ratio particles (HARPs) were fabricated as previously reported.[34,35] Briefly, 125 mg/ml solution of 45 kD PCL in trifluoroethanol was spun cast onto a glass wafer at 1000 rpm for 30 s, followed by heating at 150 °C to increase homogeneity of the surface coating. After cooling, an anodized aluminum oxide (AAO) membrane (37 mm, 200 nm pore size) was placed atop the PCL film and heated to 120 °C on a hot plate. This caused rapid cylinder formation into the AAO pores via capillary action (Figure S1). Templating was allowed to continue for 2 h, followed by removal from the hot plate and cooling of the material. The AAO templates with HARPs embedded inside the membrane were then incubated in 5 M NaOH (1 AAO disk per 10 mL NaOH) to etch the AAO template, and were shaken at room temperature for 25 minutes, followed by sonication in a bath sonicator for 10 minutes. Following AAO etching, the solution was diluted 2-fold in ddH$_2$O and centrifuged at 3000 rpm for 10 minutes to cause HARP sedimentation. NaOH supernatant

was removed and the HARPs were washed 2 times with cold ddH$_2$O, followed by PBS, and finally with 2–4 additional ddH$_2$O washes until a neutral pH was measured. HARPs were then passed through a 40 μm cell strainer to remove large aggregates and stored in ddH$_2$O at 4 °C. To fabricate fluorescent HARPs, Nile red dye was added to the PCL/TFE solution at 0.5 mg/ml prior to spin casting and templating. This PCL molecular weight and solution concentration afford HARPs of 200 nm in width and 20 μm in length. Adjusting PCL concentration and molecular weight, as well as templating times can lead to HARPs of shorter lengths.[34] HARP length was confirmed with confocal microscopy and surface charge was measured with a Malvern Zetasizer DS90.

PCL microspheres were fabricated through an oil-in-water precipitation technique. PCL (15 kD) was dissolved in acetone (10 mL) at 20 mg/ml. The solution was sonicated for 30 min to allow for the complete dissolution of PCL. A solution of Pluronic F-68 (3 mg/ml) in ddH$_2$O was prepared and stirred at 500 rpm. The PCL solution was added dropwise to the stirring aqueous solution. The solution turned opaque immediately as a result of the precipitation of PCL particles. The solution was stirred for 2 h at 30 °C to allow for acetone evaporation. The solution was then strained over a 20 μm mining mesh to filter out large particulates. The solution was centrifuged at 3000 rpm and washed into ddH$_2$O with 0.5 wt% poly(vinyl alcohol) to prevent aggregation, and lyophilized. Following lyophilization, PCL microspheres were reconstituted in ddH$_2$O and diluted 5-fold with 5 M NaOH and incubated at RT under shaking for 45 minutes to facilitate PCL surface hydrolysis and instill negative surface charge. Following incubation, the solution was filtered using a 0.2 μm spin filter and washed 3 times with cold ddH$_2$O and stored at 4 °C. Microsphere size and surface charge were measured with a Malvern Zetasizer.

Gelatin-fluorescein conjugates were prepared by incubating Gelatin Type B (20 mg/ml) and Fluorescein-NHS (10 equiv. 1.9 mg/ml) in 50 mM HEPES pH 8 overnight at room temperature while shaking. The gelatin-fluorescein conjugate was purified by multiple rounds of spin concentration (10 kD MWCO) into ddH$_2$O followed by lyophilization to yield a yellow powder (14.5 mg, 73%) Prior to microsphere fabrication, gelatin solution was prepared at 80 mg/ml in PBS with 1 mg/ml gelatin-fluorescein. The solution was heated to 40 °C to fully dissolve the gelatin and prevent gelation. Gelatin microspheres were generated using a flow-focusing microfluidic dropmaker with 40 μm nozzle. The dropmaking device was fabricated using a conventional soft lithography protocol as previously described.[49] For dropmaking, the gelatin solution was loaded into a syringe and placed on a syringe pump (New Era, catalog no. NE-501) fitted with a heating element and digital controller set to 40°C to prevent gelation in the syringe. Syringe pumps were operated at flow rates of 300 μL/h for the gelatin solution and 600 μL/h for fluorinated oil (3M, HFE-7500) containing 2% (w/w) of a PEG-PFPE block copolymer surfactant (Ran Technologies, 008-Fluoro-surfactant). Droplets were collected in a 15 mL tube on ice and incubated at 4C for 1 h to allow complete gelation. Following gelation, droplets were broken in a solution of 20% (v/v) perfluro-octanol (cat. no. 370533, Sigma-Aldrich) in HFE oil. The gelatin microspheres were then washed four times in 10 mL of cold PBS before use in experiments.

4.3. Layer-by-Layer Functionalization of Particles:

The LbL functionalization of particles was conducted using chitosan (positive charge) and heparin (negative charge). Chitosan was always used as the first layer, owing to the negative surface charge of the HARPs or PCL microspheres. Chitosan (90% deacylated) was dissolved at 10 mg/ml in 0.25% acetic acid solution and incubated at 37 °C for 10–15 min to allow for complete dissolution and prevent gelation. Chitosan solution was then diluted to 2 mg/ml in a specially prepared LbL buffer (25 mM HEPES pH 7, 20 mM NaCl, 0.025% AcOH) adapted from a recent report.[53] PCL HARPs or microparticles were then reconstituted at 1 mg/ml in LbL buffer (500 μL) and added to equal volume of chitosan solution under sonication. The solution was removed from sonication after 10–15 s and shaken at room temperature for 30 min followed by multiple rounds of centrifugation and washing with ddH$_2$O. Subsequent layering with heparin or chitosan was conducted in LbL buffer using identical protocols and 2 mg/ml stock solutions of polymer.

To load FGF2 onto LbL HARPs, heparin was first co-incubated for 1 h with FGF2 at a 2:1 mass ratio heparin:FGF2 in 20 mM Na-acetate pH 6. Chitosan-HARPs were fabricated as described above and washed into ddH$_2$O, followed by incubation with equal volume of FGF2-heparin solution. No sonication was conducted during or after incubation with FGF2 to prevent protein degradation. FGF2 loading was evaluated by centrifugation of FG2-HARP solutions and measurement of FGF2 concentration in supernatant using a micro-BCA assay (ThermoFisher, Waltham, MA). Loading levels were determined by subtracting supernatant concentrations from total concentrations in solution to determine the amount of FGF2 loaded onto HARPs. Following FGF2 loading, a subsequent layer of chitosan could be deposited onto FGF2-HARPs in Na-acetate solution. HARPs were then washed into PBS for release kinetics or cell proliferation studies.

4.4. Particle and Cell Distribution Studies:

All distribution studies were measured using a Nikon Ti spinning disk confocal microscope and images were analyzed with FIJI. Fluorescent particles (PCL microspheres, PCL HARPs, and/or gelatin microspheres) were suspended in PBS and added to 96 well glass bottom plates (100 μL per well). After 3 h incubation at room temperature, solutions were imaged via fluorescence confocal microscopy. Nile red particles were imaged at the Cy3 channel, while gelatin microspheres were imaged at the FITC channel, with little to no fluorescent cross-over observed between channels. MIN6 fluorescence was imaged in the mCherry channel. All images were measured at the exact center of the well. To analyze z-axis distribution, a z-axis profile was plotted with FIJI and the raw data were exported. The minimum fluorescence value across all z stacks was subtracted as background from all images of a single sample. Percent maximum fluorescence was then calculated by dividing each fluorescence value by the maximum fluorescence value observed across all z stacks of a single sample. Percent xy areas were calculated in FIJI for GelMS particles after setting a mean GelMS fluorescence threshold for all images.

4.5. Cell Culture and Proliferation Studies:

MIN6-mCherry cells were developed in a previously described report.[15] MIN6 cells and NIH 3T3 fibroblasts were cultured in high glucose Dulbecco's Modified Eagle Medium

(DMEM) with L-glutamine, supplemented with 10% fetal bovine serum (FBS) for MIN6 or fetal calf serum (FCS) for 3T3s and penicillin/streptomycin, and incubated at 37 °C and 5% CO_2. For cell distribution studies, MIN6 cells were trypsinized and reconstituted in cell media at 2×10^6 cells/mL. Cells were then incubated with equal volumes of either media or Chit-HARPs suspended in media at 4 mg/ml. Following mixing of cells and HARPs, the mixtures were plated in triplicate in 96 well glass bottom plates (100 μL per well) for 100,000 cells per well and 2 mg/ml HARP. Cell solutions were incubated at 37 °C for 3 d, followed by fluorescence microscopic analysis of suspensions. After microscopic analysis, the overall fluorescence of the wells was measured using a SpectraMax plate reader for mCherry fluorescence at ex/em 590/610 nm to provide a readout of cell viability in accordance with previous literature.[15]

NIH 3T3 fibroblasts were used to study the efficacy of FGF2-HARP scaffolds in promoting cell proliferation. FGF2-HARPs were fabricated as described in section 4.3 and loading levels were evaluated using a micro-BCA assay. FGF2-HARPs were added to a solution of Chit-HARPs to achieve 200 ng/ml FGF2 and 2 mg/ml HARP concentrations. GelMS particles were added for a final concentration of 0.67 mg/ml. All treatment groups were suspended in phenol red free DMEM starvation media (0.5% FCS) and plated at 100 μL per well in a 96 well plate, corresponding to 20 ng FGF2, 200 μg HARP, and 67 μg GelMS per well. Treatment groups were incubated for 24 h at 37 °C to allow for dissolution of GelMS and increased suspension of HARPs. Following pre-incubation of treatment groups, NIH 3T3 fibroblasts (20 μL of 20,000 cells) were added atop treatment suspensions and all groups were incubated for an additional 3 d at 37 °C. Wells were pelleted to recover cells that weren't adhered onto the bottom of the plates and frozen at −80 °C for at least 4 h, followed by cell proliferation analysis via Cyquant Proliferation Assay (ThermoFisher, Waltham, MA), according to manufacturer instructions. For all cell studies, blanks were measured and subtracted for each treatment group without cells to account for any background fluorescence.

Supplementary Material

Refer to Web version on PubMed Central for supplementary material.

Acknowledgements

References

[1]. Daly AC, Riley L, Segura T, Burdick JA, Hydrogel microparticles for biomedical applications. Nat. Rev. Mater 2020, 5, 20–43.

[2]. Webber MJ, Berns EJ, Stupp SI, Supramolecular nanofibers of peptide amphiphiles for medicine. Isr. J. Chem 2013, 53, 530–554. [PubMed: 24532851]

[3]. Kearney CJ, Mooney DJ, Nat. Mater 2013, 12, 1004. [PubMed: 24150418]

[4]. Madl CM, Lesavage BL, Dewi RE, Dinh CB, Stowers RS, Khariton M, Lampe KJ, Nguyen D, Chaudhuri O, Enejder A, Heilshorn SC, Nat. Mater 2017, 16, 1233. [PubMed: 29115291]

[5]. Tong X, Yang F, Adv. Healthc. Mater 2018, 7, 1.

[6]. Guan X, Avci-Adali M, Alarçin E, Cheng H, Kashaf SS, Li Y, Chawla A, Jang HL, Khademhosseini A, Development of hydrogels for regenerative engineering. Biotechnol. J 2017, 12.

[7]. Sahoo JK, VandenBerg MA, Webber MJ, Adv. Drug Deliv. Rev 2017, 127, 185. [PubMed: 29128515]

[8]. Grosskopf AK, Roth GA, Smith AAA, Gale EC, Hernandez HL, Appel EA, Bioeng. Transl. Med 2020, 5, 1.

[9]. Webber MJ, Appel EA, Meijer EW, Langer R, Supramolecular biomaterials. Nat. Mater 2015, 15, 13–26.

[10]. Stapleton LM, Steele AN, Wang H, Lopez Hernandez H, Yu AC, Paulsen MJ, Smith AAA, Roth GA, Thakore AD, Lucian HJ, Totherow KP, Baker SW, Tada Y, Farry JM, Eskandari A, Hironaka CE, Jaatinen KJ, Williams KM, Bergamasco H, Marschel C, Chadwick B, Grady F, Ma M, Appel EA, Woo YJ, Nat. Biomed. Eng 2019, 3, 611. [PubMed: 31391596]

[11]. Caldwell AS, Aguado BA, Anseth KS, Adv. Funct. Mater 2019, 1907670, 1.

[12]. Griffin DR, Weaver WM, Scumpia PO, Di Carlo D, Segura T, Nat. Mater 2015, 14, 737. [PubMed: 26030305]

[13]. Han LH, Lai JH, Yu S, Yang F, Biomaterials 2013, 34, 4251. [PubMed: 23489920]

[14]. Beniash E, Hartgerink JD, Storrie H, Stendahl JC, Stupp SI, Acta Biomater. 2005, 1, 387. [PubMed: 16701820]

[15]. Nyitray CE, Chang R, Faleo G, Lance KD, Bernards DA, Tang Q, Desai TA, ACS Nano 2015, 9, 5675. [PubMed: 25950860]

[16]. Chang R, Faleo G, Russ HA, Parent AV, Elledge SK, Bernards DA, Allen JL, Villanueva K, Hebrok M, Tang Q, Desai TA, ACS Nano 2017, 11, 7747. [PubMed: 28763191]

[17]. Wang Q, Wang L, Detamore MS, Berkland C, Adv. Mater 2008, 20, 236.

[18]. Clarke KC, Douglas AM, Brown AC, Barker TH, Lyon LA, Curr. Opin. Colloid Interface Sci 2013, 18, 393.

[19]. Dugyala VR, Daware SV, Basavaraj MG, Soft Matter 2013, 9, 6711.

[20]. Riley L, Schirmer L, Segura T, Curr. Opin. Biotechnol 2019, 60, 1. [PubMed: 30481603]

[21]. Zhao Z, Ukidve A, Krishnan V, Mitragotri S, Adv. Drug Deliv. Rev 2019, 143, 3. [PubMed: 30639257]

[22]. Finbloom JA, Sousa F, Stevens MM, Desai TA, Adv. Drug Deliv. Rev 2020.

[23]. Hou S, Niu X, Li L, Zhou J, Qian Z, Yao D, Yang F, Ma PX, Fan Y, Biomaterials 2019, 223.

[24]. McCullen SD, Autefage H, Callanan A, Gentleman E, Stevens MM, Tissue Eng. Part A 2012, 18, 2073. [PubMed: 22655795]

[25]. Keane TJ, Horejs CM, Stevens MM, Adv. Drug Deliv. Rev 2018, 129, 407. [PubMed: 29425770]

[26]. Rieger KA, Birch NP, Schiffman JD, J. Mater. Chem. B 2013, 1, 4531. [PubMed: 32261196]

[27]. Nasajpour A, Mandla S, Shree S, Mostafavi E, Sharifi R, Khalilpour A, Saghazadeh S, Hassan S, Mitchell MJ, Leijten J, Hou X, Moshaverinia A, Annabi N, Adelung R, Mishra YK, Shin SR, Tamayol A, Khademhosseini A, Nano Lett. 2017, 17, 6235. [PubMed: 28819978]

[28]. Shukla S, Eber FJ, Nagarajan AS, DiFranco NA, Schmidt N, Wen AM, Eiben S, Twyman RM, Wege C, Steinmetz NF, Adv. Healthc. Mater 2015, 4, 874. [PubMed: 25641794]

[29]. Kinnear C, Moore TL, Rodriguez-Lorenzo L, Rothen-Rutishauser B, Petri-Fink A, Chem. Rev 2017, 117, 11476. [PubMed: 28862437]

[30]. Geng Y, Dalhaimer P, Cai S, Tsai R, Tewari M, Minko T, Discher DE, Nat. Nanotechnol 2007, 2, 249. [PubMed: 18654271]

[31]. Finbloom J, Aanei I, Bernard J, Klass S, Elledge S, Han K, Ozawa T, Nicolaides T, Berger M, Francis M, Nanomaterials 2018, 8, 1007.

[32]. Pinney JR, Du KT, Ayala P, Fang Q, Sievers RE, Chew P, Delrosario L, Lee RJ, Desai TA, Biomaterials 2014, 35, 8820. [PubMed: 25047625]

[33]. Le LV, Mohindra P, Fang Q, Sievers RE, Mkrtschjan MA, Solis C, Safranek CW, Russell B, Lee RJ, Desai TA, Biomaterials 2018, 169, 11. [PubMed: 29631164]

[34]. Zamecnik CR, Lowe MM, Patterson DM, Rosenblum MD, Desai TA, ACS Nano 2017, 11, 11433. [PubMed: 29124929]

[35]. Zamecnik CR, Levy ES, Lowe MM, Zirak B, Rosenblum MD, Desai TA, Biomaterials 2020, 230.

[36]. Hernández AR, Contreras OC, Acevedo JC, Moreno LGN, Am. J. Polym. Sci 2013, 3, 70.

[37]. Sun H, Önneby S, Polym. Int 2006, 55, 1336.

[38]. Correa S, Dreaden EC, Gu L, Hammond PT, Control J. Release 2016, 240, 364.

[39]. Dai T, Tanaka M, Huang YY, Hamblin MR, Chitosan preparations for wounds and burns: Antimicrobial and wound-healing effects. Expert Rev. Anti. Infect. Ther 2011, 9, 857–879. [PubMed: 21810057]

[40]. Belair DG, Le NN, Murphy WL, Chem. Commun 2014, 50, 15651.

[41]. Chen M, Runge T, Wang L, Li R, Feng J, Shu XL, Shi QS, Carbohydr. Polym 2018, 200, 115. [PubMed: 30177147]

[42]. De Stefano C, Gianguzza A, Piazzese D, Sammartano S, Chem. Speciat. Bioavailab 2010, 22, 99.

[43]. Leduc J-F, Leduc R, Cabana H, Adsorpt. Sci. Technol 2014, 32, 557.

[44]. Nyitray CE, Chang R, Faleo G, Lance KD, Bernards DA, Tang Q, Desai TA, ACS Nano 2015, 9, 5675. [PubMed: 25950860]

[45]. Lewis JS, Stewart JM, Marshall GP, Carstens MR, Zhang Y, Dolgova NV, Xia C, Brusko TM, Wasserfall CH, Clare-Salzler MJ, Atkinson MA, Keselowsky BG, ACS Biomater. Sci. Eng 2019, 5, 2631. [PubMed: 31119191]

[46]. Allen R, Chizari S, Ma JA, Raychaudhuri S, Lewis JS, ACS Appl. Bio Mater 2019, 2, 2388.

[47]. Afewerki S, Sheikhi A, Kannan S, Ahadian S, Khademhosseini A, Bioeng. Transl. Med 2019, 4, 96. [PubMed: 30680322]

[48]. Nguyen AH, McKinney J, Miller T, Bongiorno T, McDevitt TC, Acta Biomater. 2015, 13, 101. [PubMed: 25463489]

[49]. Demaree B, Weisgerber D, Lan F, Abate AR, J. Vis. Exp 2018, 2018.

[50]. Samy KE, Levy ES, Phong K, Demaree B, Abate AR, Desai TA, Sci. Rep 2019, 9, 1. [PubMed: 30626917]

[51]. Dvorak P, Bednar D, Vanacek P, Balek L, Eiselleova L, Stepankova V, Sebestova E, Kunova Bosakova M, Konecna Z, Mazurenko S, Kunka A, Vanova T, Zoufalova K, Chaloupkova R, Brezovsky J, Krejci P, Prokop Z, Dvorak P, Damborsky J, Biotechnol. Bioeng 2018, 115, 850. [PubMed: 29278409]

[52]. Beenken A, Mohammadi M, The FGF family: Biology, pathophysiology and therapy. Nat. Rev. Drug Discov 2009, 8, 235–253. [PubMed: 19247306]

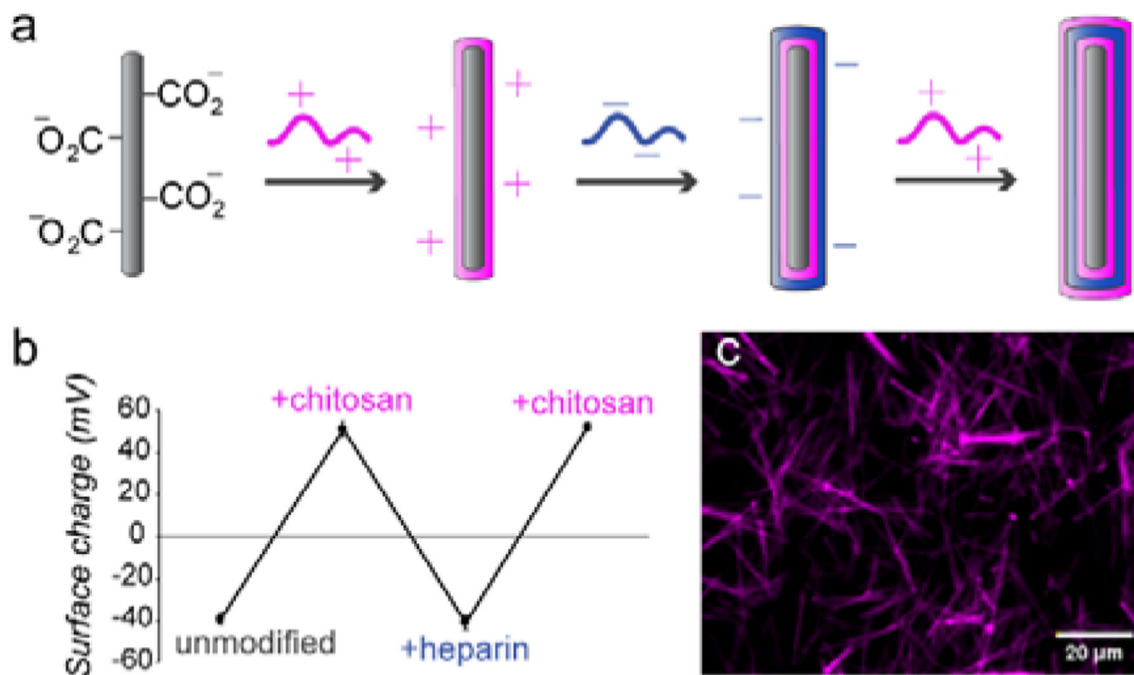[53]. Correa S, Boehnke N, Deiss-Yehiely E, Hammond PT, ACS Nano 2019, 13, 5623. [PubMed: 30986034]

Figure 1.
Functionalization of polycaprolactone high aspect ratio particles (HARPs) via layer-by-layer electrostatic assembly. (a) HARPs bearing negative charge are functionalized with charged biopolymers such as chitosan (positive charge) and heparin (negative charge) for layer-by-layer assembly. (b) Zeta potential measurements of HARPs confirm chitosan and heparin deposition, as demonstrated through observed surface charge oscillation. (c) Fluorescent microscopy of HARPs loaded with Nile red dye in the hydrophobic polymer core of the particles.
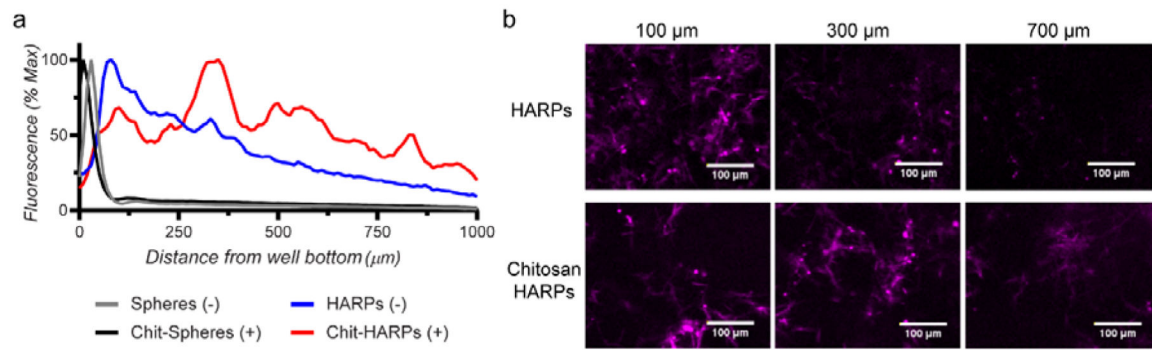
Figure 2.
Physicochemical properties of PCL colloids influence particle suspension behaviors. (a) Overall z-axis distribution of fluorescent PCL spheres and HARPs of positive or negative charge in PBS solutions. (b) Representative fluorescent microscope images of negatively charged HARPs and positively charged Chitosan-HARPs at z positions of 100, 300, and 700 μm from the well bottom.
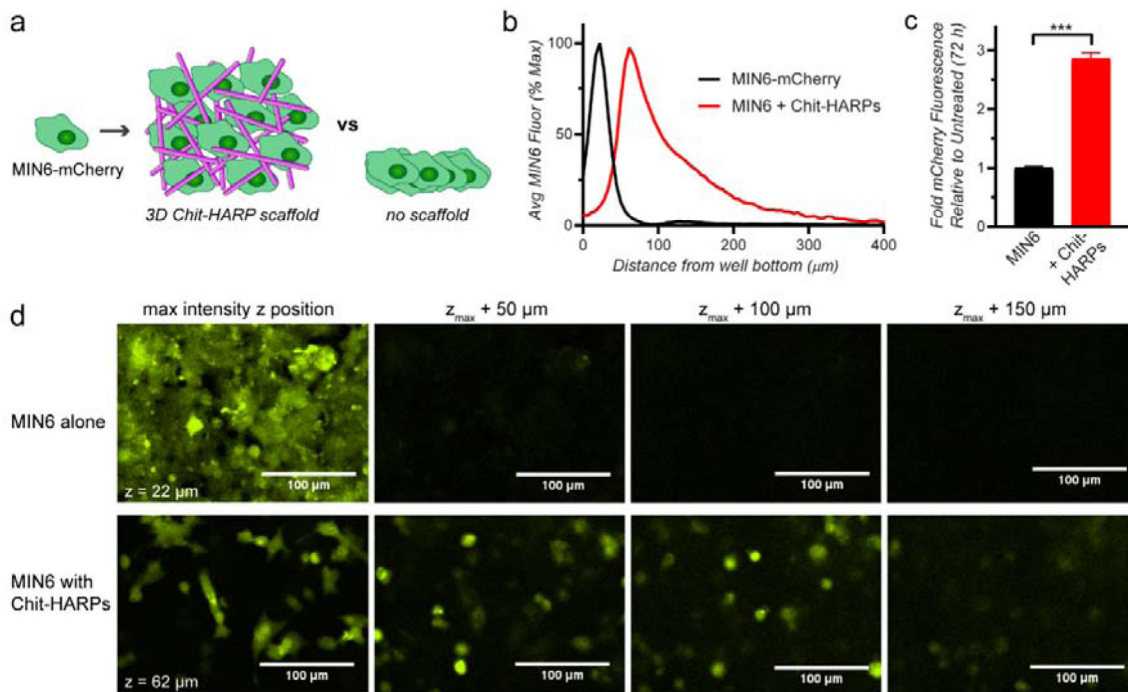
Figure 3.
Chitosan-HARP scaffolds stabilize cellular suspensions for therapeutic cell delivery. (a) Schematic of 3D cell suspensions within Chit-HARP scaffolds, which prevent the cell sedimentation and aggregation commonplace without scaffolds. (b) Average z-axis distribution of fluorescent MIN6-mCherry cells alone or with Chit-HARPs following 3 d incubation (n = 3). Statistically significant differences (p < 0.01) in distribution were observed for all z slices with the exception of z = 38 μm. (c) Total mCherry fluorescence for MIN6 with or without Chit-HARP scaffolds after 3 d. ***p < 0.001. (d) Microscopy images of MIN6 cells at maximum fluorescent intensity z positions with and without Chit-HARP scaffolds, as well as representative images at z_{max} + 50, 100, 150 μm.
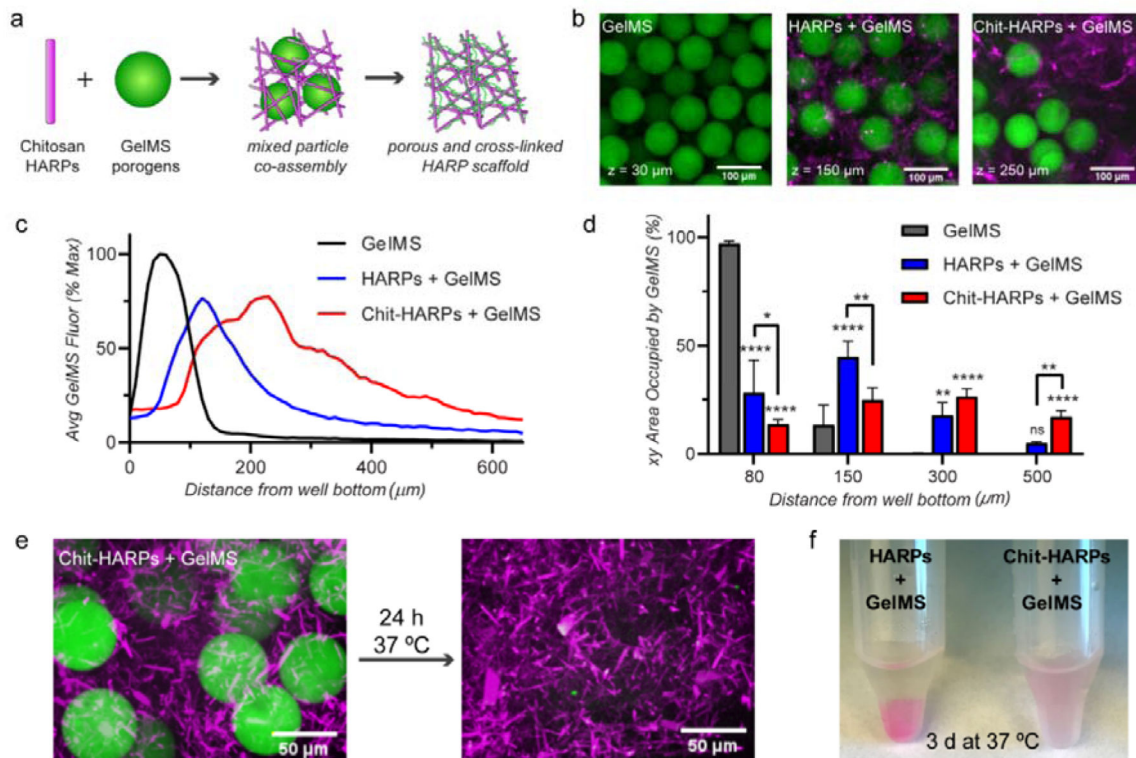
Figure 4.
HARP scaffolds stabilize mixed particle assemblies through HARP network formation and electrostatic interactions. (a) Chitosan-coated HARPs co-assemble with gelatin microsphere (GelMS) porogens to form a mixed particle assembly. Following GelMS dissolution at 37 °C, Chit-HARP scaffolds remain as porous suspensions through proposed gelatin-HARP electrostatic crosslinking. (b) Fluorescence confocal microscopy images of GelMS, HARPs + GelMS, and Chit-HARPs + GelMS assemblies in PBS after 3 h, at respective maximum fluorescence z positions. (c) GelMS porogen z-axis distribution for GelMS alone or in co-assembly systems after 3 h. (d) GelMS distribution in the xy plane at various heights. Significant differences in % xy area occupancy were observed between both co-assembly systems vs GelMS alone, as well as between HARP vs Chit-HARP co-assembly systems. *$p<0.05$. **$p<0.01$. ***$p<0.001$. ****$p<0.0001$. (e) 3D z-axis projections of Chit-HARPs + GelMS after 3 h and 24 h incubation at 37 °C in PBS. GelMS porogen dissolution was observed after 24 h incubation via fluorescence microscopy. (f) Macroscopic analysis of HARP + GelMS vs Chit-HARP + GelMS co-assemblies after 3 d incubation at 37 °C.
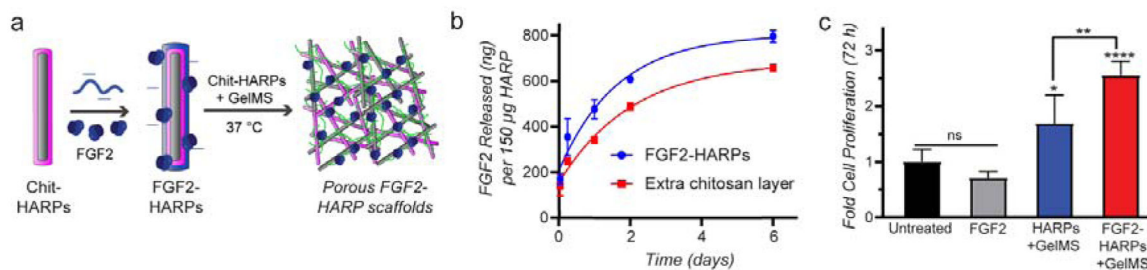
Figure 5.
FGF2-functionalized HARPs co-assembled with GelMS improve fibroblast activation and proliferation. (a) Fibroblast growth factor 2 (FGF2) was pre-incubated with heparin to form FGF2-heparin complexes and was successfully loaded onto Chit-HARPs through LbL assembly with over 50% loading efficiency. FGF2-HARPs were mixed with Chit-HARPs and GelMS to facilitate porous and stable FGF2-HARP suspensions following GelMS dissolution. (b) FGF2 release from HARP scaffolds. First order release kinetics were observed over 6 days release. Release kinetics were slowed following addition of chitosan onto FGF2-HARPs. (c) NIH-3T3 fibroblast proliferation when cultured on top of scaffolds pre-incubated for 24 h. FGF2 and FGF2-HARP groups contained 20 ng of growth factor per well. Statistical analysis performed via one-way ANOVA with multiple comparisons. * $p < 0.05$, ** $p < 0.01$, **** $p < 0.0001$.